Multiscale analysis of tree cover and aboveground carbon stocks in pinyon–juniper woodlands

Cho-Ying Huang,[1,2,5] Gregory P. Asner,[1] Roberta E. Martin,[1] Nichole N. Barger,[3] and Jason C. Neff[4]

[1]*Department of Global Ecology, Carnegie Institution for Science, 260 Panama Street, Stanford, California 94304 USA*
[2]*Department of Geomatics, National Cheng Kung University, 1 University Road, Tainan 70101 Taiwan*
[3]*Department of Ecology and Evolutionary Biology, University of Colorado, Boulder, Colorado 80309 USA*
[4]*Geological Sciences and Environmental Studies Departments, University of Colorado, Boulder, Colorado 80309 USA*

Abstract. Regional, high-resolution mapping of vegetation cover and biomass is central to understanding changes to the terrestrial carbon (C) cycle, especially in the context of C management. The third most extensive vegetation type in the United States is pinyon–juniper (P–J) woodland, yet the spatial patterns of tree cover and aboveground biomass (AGB) of P–J systems are poorly quantified. We developed a synoptic remote-sensing approach to scale up pinyon and juniper projected cover (hereafter "cover") and AGB field observations from plot to regional levels using fractional photosynthetic vegetation (PV) cover derived from airborne imaging spectroscopy and Landsat satellite data. Our results demonstrated strong correlations ($P < 0.001$) between field cover and airborne PV estimates ($r^2 = 0.92$), and between airborne and satellite PV estimates ($r^2 = 0.61$). Field data also indicated that P–J AGB can be estimated from canopy cover using a unified allometric equation ($r^2 = 0.69$; $P < 0.001$). Using these multiscale cover–AGB relationships, we developed high-resolution, regional maps of P–J cover and AGB for the western Colorado Plateau. The P–J cover was 27.4% ± 9.9% (mean ± SD), and the mean aboveground woody C converted from AGB was 5.2 ± 2.0 Mg C/ha. Combining our data with the southwest Regional Gap Analysis Program vegetation map, we estimated that total contemporary woody C storage for P–J systems throughout the Colorado Plateau (113 600 km^2) is 59.0 ± 22.7 Tg C. Our results show how multiple remote-sensing observations can be used to map cover and C stocks at high resolution in drylands, and they highlight the role of P–J ecosystems in the North American C budget.

Key words: AVIRIS; ETM+; Juniperus osteosperma; *Landsat; multiscale analyses; North American Carbon Program;* Pinus edulis; *remote sensing; scaling.*

Introduction

Arid and semiarid environments (known collectively as "drylands") cover about 3.4×10^6 km^2 of North America (Asner et al. 2004). During the past century, one of the most significant directional vegetation changes in drylands has been woody encroachment, or the shifting of lifeform dominance from herbaceous to woody plants (Glendening 1952, Buffington and Herbel 1965, Branson 1985, Archer 1993, Archer et al. 1995). Recent syntheses suggested that woody encroachment contributes significantly to a North American carbon (C) sink (Houghton et al. 1999, Schimel et al. 2000, Pacala et al. 2001). However, Jackson et al. (2002) provided evidence that C losses may occur with woody encroachment in grassland ecosystems. In addition, increased perturbations such as drought and wildfire resulting from climate anomalies (Breshears et al. 2005)

or nonnative species (Bradley et al. 2006) might lead to a reduction of woody plants and conversion of a C sink to a C source. These changes are difficult to assess regionally due to the heterogeneity of woody vegetation in most dryland regions (Ben-Shahar 1998, Bond and Midgley 2001, Augustine and McNaughton 2004). Any regional analysis of change is thus hampered by our poor understanding of woody cover and biomass.

While our regional knowledge of contemporary woody cover and biomass distributions is crude, what we do know largely comes from studies focused on creosotebush (*Larrea tridentata*), mesquite (*Prosopis* spp.), and/or oak woodlands (*Quercus* spp.) in arid and semiarid regions (McClaran and McPherson 1999, Huenneke et al. 2002, Hughes et al. 2006). Pinyon–juniper (P–J) woodlands are the third largest vegetation type in the United States, much of which occurs across public lands managed by the Bureau of Land Management and other agencies. As a result, management of these ecosystems over the longer term may significantly impact ecosystem C stocks across drylands of the western United States.

Land-use changes, such as the introduction of domestic livestock across the western United States in

---

the mid-1800s and subsequent changes in fire regimes, are key factors mediating woody plant proliferation (Barney and Frischknecht 1974, Miller and Rose 1999, West 1999, Asner et al. 2004). Studies of stand age structure in P–J woodlands provide evidence that much of the recruitment has occurred in the last century. In Utah, more than half of the P–J tree stands were in the 40–120 year age range, with only 20% of stands dating to >200 years (O'Brien and Woudenberg 1999). Climate patterns over the last century may also be an important factor determining recently observed changes in P–J woodland populations (Miller and Wigand 1994, Gray et al. 2006). P–J woodland expansion has been observed at remote sites on the Colorado Plateau that were historically inaccessible to domestic livestock or fire suppression activities (Tausch and Nowak 1999, Harris et al. 2003).

Pinyon–juniper woodlands are not only a spatially extensive vegetation type in the United States, but also have high levels of biomass relative to other dryland woody plant communities. At maximum stand densities, P–J systems can maintain biomass and net primary production (NPP) levels 2–4 times that of more intensively studied mesquite and oak woodlands, and 10 times that of creosote shrublands (Whittaker and Niering 1975, Gholz 1982, Grier et al. 1992, Hibbard et al. 2001, Hughes et al. 2006). However, there is a lack of information on the current spatial patterns of tree cover and C stocks in P–J woodlands, an area of ~113 600 km^2 throughout the Colorado Plateau (Lowry et al. 2007).

Remote sensing has proven difficult for deriving woody cover over vast arid and semiarid environments (Scanlon et al. 2002, Goslee et al. 2003, Weisberg et al. 2007). Spectral mixture analysis techniques are now commonly used to derive the fractional cover of photosynthetic vegetation (PV) from airborne imaging spectroscopy (e.g., Airborne Visible and Infrared Imaging Spectrometer, AVIRIS; Asner and Heidebrecht 2005), and the PV fraction is primarily contributed by woody vegetation when the data are acquired during the dry season, a time when the majority of herbaceous plants are senescent (Asner et al. 2003a). Numerous studies have demonstrated that woody cover is a strong predictor of woody biomass at the scale of individual canopies and plots in dryland ecosystems (Ludwig et al. 1975, Chojnacky 1991, Asner et al. 2003a, Miller et al. 2003, Barbosa and Fearnside 2005, Northup et al. 2005, Huang et al. 2007). Therefore, correlating dry-season PV fraction with field observations would permit relatively broad-scale estimation of woody biomass. However, a major pitfall in such an approach is that the geographic coverage of airborne hyperspectral images is relatively small, and they are not sufficient to monitor very large regions (e.g., >10 000 km^2). The issue of spatial coverage could be resolved by substituting airborne hyperspectral images with satellite multispectral data. However, the accuracy of the dryland PV fraction derived from multispectral images is questionable due to insufficient spectral channels required to quantify PV from other land surface components (or endmembers) such as nonphotosynthetic vegetation (e.g., litter) and soils (Asner and Heidebrecht 2002).

The objective of this study was to develop a multiscale approach to link P–J cover (the percentage of ground surface covered when P–J canopies are viewed planometrically) and aboveground biomass (AGB) observations from field measurements to small regional-scale estimates from airborne hyperspectral imaging, and upward to large regional estimates from satellite multispectral observations. We applied this new approach to estimate the current-day tree cover and AGB in P–J systems of the Colorado Plateau. A large-scale analysis of P–J cover and AGB spatial patterns in different terrains was also conducted to demonstrate the significance of the derived P–J maps.

METHODS

Study region

Our study focused on 30 500 km^2 of pinyon–juniper woodlands of the western Colorado Plateau covering Grand Canyon and Zion National Parks and Grand Staircase-Escalante National Monument (Fig. 1), an area comprising 27% of the Colorado Plateau. The spatial extent of P–J woodlands was first estimated from the southwest Regional Gap Analysis Program (ReGAP) vegetation coverage (Lowry et al. 2007). The elevation of P–J ecosystems within the site is 1852 ± 232 m (mean ± SD). The climate is semiarid with wet cool winters and dry hot summers (Fig. 2b). Annual precipitation and temperature are ~307.1 ± 95.1 mm and 14.7° ± 0.5°C (mean ± SD), respectively, according to seven years (2000–2006) of climate records from 28 National Climatic Data Center stations (Fig. 1). P–J woodlands occur across a wide range of soil and geologic types with previous studies showing no correlation between the spatial extent of P–J woodlands and geological substrates originated from different parent materials (e.g., granite, limestone, volcanic material; McPherson 1997).

Dominant overstory plants in P–J ecosystems are pinyon pines (e.g., *Pinus edulis*, *P. monophylla*, *P. cembroides*) and junipers (e.g., *Juniperus deppeana*, *J. monosperma*, *J. occidentalis*, *J. osteosperma*), but the abundance of each species varies across the region (Grier et al. 1992, West 1999). Dominant tree species at our study region are *P. edulis* and *J. osteosperma* with a diverse array of understory plant communities occurring in association with the P–J overstory (West 1999). Phenology of P–J woodlands can be illustrated by referring to time-series MODIS–NDVI (the Moderate Resolution Imaging Spectroradiometer–Normalized Difference Vegetation Index; Fig. 2a). MODIS is a satellite instrument (data *available online*),[6] and the NDVI is a metric highly correlated with photosynthetic

---

[6] ⟨http://modis.gsfc.nasa.gov/⟩
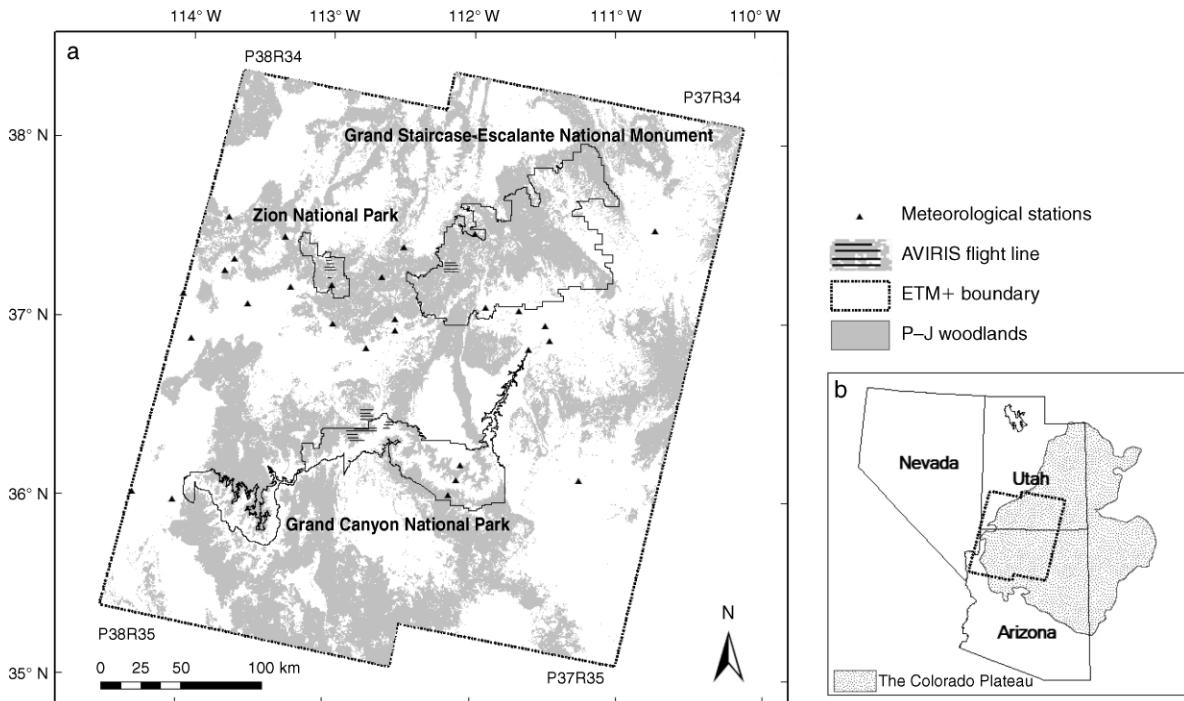
FIG. 1. (a) The boundaries of four Enhanced Thematic Mapper Plus (ETM+) images based on the Landsat Worldwide Reference System (the dotted outline) and two national parks and one national monument (solid outlines). Airborne Visible/Infrared Imaging Spectrometer (AVIRIS) flight lines from 2003 are shown as short solid lines; the triangles are the National Climatic Data Center meteorological stations ($n = 28$). The gray areas are pinyon–juniper (P–J) woodlands defined by the southwest Regional Gap Analysis Program. (b) The location of the study site within three southwestern states (USA), and the boundary of the Colorado Plateau (the dotted polygon).
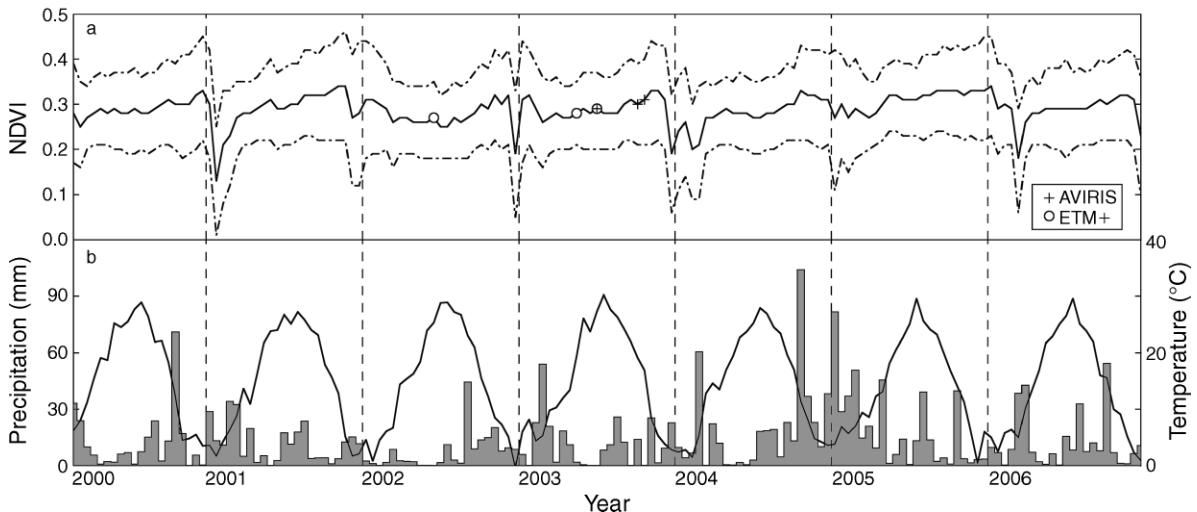
FIG. 2. (a) Phenology of pinyon–juniper woodlands within the study area derived from seven years (2000–2006) of the Moderate Resolution Imaging Spectroradiometer-Normalized Difference Vegetation Index (MODIS-NDVI) time-series data; the solid and dash-dotted lines, respectively, define the mean ± SD. Acquisition time periods (during 2002 and 2003) of Airborne Visible/Infrared Imaging Spectrometer (AVIRIS) and Enhanced Thematic Mapper Plus (ETM+), respectively, are shown as plus signs and circles. (b) Biweekly (16-day MODIS period) precipitation (gray bars) and temperature (solid line) according to daily records from 28 National Climatic Data Center meteorological stations within the study site (Fig. 1a).

activity and associated greenness (Tucker and Sellers 1986). We show these MODIS data to illustrate that there was no pronounced seasonal phenological cycle during our study period, which was typical of conifers (also see Rich et al. [2008]). This is critical because we combine data from multiple time periods.

Field measurements

Field campaigns were conducted during the summer (May–September) of 2005. Photosynthetic vegetation (PV) cover was measured at 20 P–J sites in northern Arizona and southern Utah across different soil types and land-use histories within the AVIRIS campaign region (Fig. 1a). The elevation range of these sites was 1716–2184 m. At each site, a 100-m transect was randomly established, and covers (PV, litter, and soil) were measured in 10-cm increments using a line-intercept method (Canfield 1941). During the campaigns, we observed that the majority of herbaceous plants were senescent and PV consisted mainly of P–J cover. AGB (kg) of P–J was determined through a nondestructive method by using previously established allometrics (Darling 1967) based on root collar diameter (RCD, cm). RCD is a measure of the sum of each stem diameter at the ground level (Grier et al. 1992). RCD is specifically designed for measuring trees with multiple stems such as *P. edulis* and *J. osteosperma*. The allometric equations for these two species are

$$AGB_{PIED} = 0.024RCD_{PIED}^{2.67} \qquad (1)$$

$$AGB_{JUOS} = 0.013RCD_{JUOS}^{2.81}. \qquad (2)$$

The subscripts PIED and JUOS in Eqs. 1 and 2 are *P. edulis* and *J. osteosperma*, respectively. The allometric equations are typical for P–J woodlands within the study region derived from destructive harvesting of *P. edulis* (*n* = 10) and *J. osteosperma* (*n* = 9) in Grand Canyon National Park encompassing a wide range of RCD size classes. There was an excellent fit based upon visual assessment of these models (note that no r^2 was reported in Darling [1967]). We measured P–J RCD of 1450 individuals (*P. edulis* = 889 and *J. osteosperma* = 561) across a wide range of topoedaphic conditions within the study site. Canopy cover has also proven to be a significant predictor of woody AGB in drylands (North-up et al. 2005), and can be directly derived from remotely sensed data (Asner et al. 2003a, Huang et al. 2007). Hence, canopy cover for each individual sampled tree was computed as a circle, whose radius was half of its longest axis. The correlation between RCD and canopy cover for *P. edulis* and *J. osteosperma* was used to derive P–J AGB directly from cover.

Remote sensing

AVIRIS (Green et al. 1998) and spaceborne multispectral Landsat Enhanced Thematic Mapper Plus (ETM+) images were used in this study. AVIRIS was flown twice over the national parks and the national monument during early summer and mid-fall (Grand Canyon = 3 July and 17 October; Grand Staircase-Escalante = 3 July and 9 October; Zion = 6 July and 9 October) of 2003. ETM+ data were also collected during the similar dry period of 2002 (Landsat Worldwide Reference System P37R34 = 12 June) or 2003 (P37R35 = 9 July; P38R34 = 30 June; P38R35 = 21 May; Figs. 1 and 2a). During these hot, dry periods, most herbaceous plants were senescent according to our field observations. Therefore, the majority of fractional PV cover extracted from AVIRIS and ETM+ would be mainly contributed from P–J cover. The study area extent was 296 km² for AVIRIS and 107 209 km² for ETM+. The data acquisition time for AVIRIS was approximately solar noon (11:13–13:54 local time), and for ETM+ it was 10:47 local time.

AVIRIS was flown on a Twin Otter aircraft at an altitude of 3600 m above ground level, resulting in image pixel resolution (ground sample distance) of 3.6 m. The imagery was collected in the east–west direction, and geo-registration was processed by Jet Propulsion Laboratory (information *available online*).[7] AVIRIS measures upwelling radiance in the 400–2500 nm wavelength range through the visible, near-infrared, and shortwave infrared region at a sampling interval of ~10 nm. The four cloud-free ETM+ images were acquired from the U.S. Geological Survey (*available online*).[8] ETM+ is a multispectral spaceborne sensor with six bands covering the visible, near-infrared, and shortwave infrared spectral regions with a nominal spatial resolution of 30 m, plus one thermal 60-m band. The ETM+ images were orthorectified using a digital elevation model (DEM). The AVIRIS images were converted from raw digital counts to apparent surface reflectance (unitless, ranging from zero to one) using ACORN Version 5.05 (ImSpec, Palmdale, California, USA). ACORN can be run in hyperspectral mode (for AVIRIS) to estimate atmospheric water vapor content from the data. ACORN input parameters for this mode included aircraft altitude above ground, visibility (aerosol), and time of day. The ETM+ images were processed using the 6S model (Vermote et al. 1997). In 6S, we used the mean aerosol optical thickness and water vapor content for the month in which the image data were collected. These mean values were acquired from the 1 × 1° monthly global products from the moderate resolution imaging spectroradiometer (MODIS). A detailed procedure of ETM+ preprocessing is described in Asner et al. (2005a, b).

Spectral mixture analysis

Spectral mixture analysis is a technique used to derive subpixel cover fractions of surface materials collected from remotely sensed data (Adams et al. 1993). The method is ideal for use in dryland environments where subpixel cover variation is high. Each endmember

---

[7] ⟨http://aviris.jpl.nasa.gov/⟩
[8] ⟨http://glovis.usgs.gov/⟩

component contributes to the pixel-level spectral reflectance (ρ_{pixel}) as the linear combination of endmember (e) spectra:

$$\rho_{\text{pixel}} = \sum [\rho_e C_e] + \varepsilon$$

$$= [\rho_{\text{PV}} C_{\text{PV}} + \rho_{\text{litter}} C_{\text{litter}} + \rho_{\text{soil}} C_{\text{soil}}] + \varepsilon \quad (3)$$

$$\sum [C_e] = 1.0 \quad (4)$$

where ρ and C are the reflectance and cover fraction of each endmember (PV, litter, and soil), respectively, and ε is the error term (Eq. 3). Eq. 4 indicates that the endmembers sum to unity. Asner et al. (2000) found that there were a number of endmember combinations that can produce a particular spectral signal, so a wide range of numerically acceptable unmixing results for any image pixel were possible. Hence, a probabilistic spectral-mixture analysis technique, known as Automated Monte Carlo Unmixing (AutoMCU; Asner and Lobell 2000, Asner and Heidebrecht 2002) was implemented to account for this natural variability (Asner 1998, Stimson et al. 2005) through iterative random selection of endmember reflectance from "bundles" (Bateson et al. 2000). We acquired endmember bundles for PV, litter, and soils using a field spectroradiometer (Analytical Spectral Devices, Boulder, Colorado, USA) collected in arid and semiarid environments in North and South America (Asner 1998, Asner et al. 2000, Harris et al. 2003). The AVIRIS data were analyzed with AutoMCU using the tied-shortwave infrared spectra technique. The difference of spectral signatures among PV, litter, and soils is most distinguishable within a part of the shortwave infrared region (2000–2400 nm), and it can be further enhanced by "tying" these spectra at 2078 nm (Asner and Lobell 2000, Asner and Heidebrecht 2002). For ETM+ images, the AutoMCU code was used in multispectral mode, as described by Asner et al. (2003a, b).

Scaling of pinyon–juniper cover and biomass

AVIRIS pixels containing the field sampling transects were used to develop a regression between AVIRIS PV fraction (AVIRIS-PV) and P–J cover. P–J canopy cover can be derived by taking the dimension of fine resolution AVIRIS pixels into account, and AGB can then be estimated by referring to the correlation between field-measured AGB and canopy cover. P–J cover and AGB maps were then averaged using a low-pass filter and resampled to a 30-m spatial resolution using the nearest neighbor method to match with ETM+ photosynthetic vegetation (ETM-PV) fraction. Approximately 0.5% of the resampled AVIRIS P–J cover and AGB estimates and their corresponding ETM-PV pixels were randomly selected without replacement to derive scaling equations from landscape to regional levels of remote-sensing coverage. The random selection of these image-to-image pairs minimized spatial autocorrelation (Gruijter and

Braak 1990, Brus and DeGruijter 1993), affording a straightforward method for translating field-based and aircraft-based cover and biomass estimates to the regional scale of the Colorado Plateau.

Validation of remote-sensing estimates

We evaluated the performance of our large, regional P–J cover estimation by comparing to two independent sets of tree-cover data: ReGAP field plots (available online)[9] (Lowry et al. 2007) and LANDFIRE tree canopy cover product (available online).[10] The tree cover of ReGAP field plots (≥ 1 ha) was sampled mostly along secondary road networks and estimated using a visual method. The LANDFIRE product was generated using Landsat data by a regression tree with aid from small scale 1-m digital orthophoto quadrangles (DOQ; White et al. 2005). The sample correlation coefficient (r) was used to test the relationship between ReGAP and our tree-cover measures. For LANDFIRE, ~0.5% of overlapping pixels were randomly selected (without replacement) for the comparison. An ordinal logistic regression was used to investigate the correlation since the LANDFIRE product was ordinal and binned into 10% discrete incremental classes, and a mid-point (e.g., 15%) was used to represent each class. For both validation data sets, mean overall bias (our estimate minus validation) and absolute error, and their relationships with cover abundance (e.g., 1–10%, 11–20%, and so forth) were assessed.

To our knowledge, this is the first study to estimate P–J AGB storage at a large regional scale and at high spatial resolution across the Colorado Plateau. Hence, we only performed a rough comparison of means between our remote-sensing-based estimates and small-scale field observations located close to our study site (Grier et al. 1992). Note that a pixel-by-pixel comparison was not possible here due to the lack of geographical coordinates for specific field plots in past ground-based studies.

P–J variation with topography

Basic relationships between regional P–J cover and AGB and terrain complexity were analyzed. Elevation was acquired from a 30-m digital elevation model (DEM) that was originally used to orthorectify ETM+ images. Therefore, the geo-registrations for the P–J cover and AGB and DEM were seamlessly matched. Slope and aspect were derived from the DEM using ArcGIS version 9.2 (ESRI, Redlands, California, USA). Aspect was originally in degrees (°), but was assigned to nominal classes: North (0°–44° and 315°–359°), East (45°–134°), South (135°–224°), and West (225°–314°). Additionally, flat terrains (slope < 5°) without apparent facings were excluded from the analysis. P–J cover and AGB of each pixel and corresponding elevation, slope, and aspect were extracted and compared.

[9] ⟨http://ftp.nr.usu.edu/swgap/⟩
[10] ⟨http://www.landfire.gov/⟩
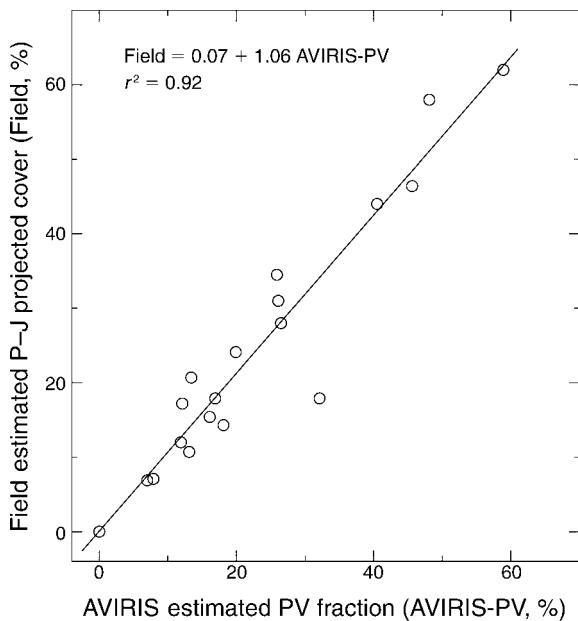
Fig. 3. The relationship between field estimated projected tree cover in pinyon–juniper (P–J) ecosystems in the Colorado Plateau and dry-season photosynthetic vegetation (PV) fractions derived from the Airborne Visible/Infrared Imaging Spectrometer (AVIRIS) images ($n = 20$).

RESULTS

AVIRIS mapping of pinyon–juniper cover and biomass

The spatial pattern of P–J cover collected from field measurements was heterogeneous (mean = 22.0%; range = 0.0–58.9%; SD = 16.1%), but was accurately estimated by high spatial resolution AVIRIS-PV ($r^2 = 0.92$; $P < 0.0001$; Fig. 3). Canopy cover was a strong indicator ($P < 0.0001$, log–log relationship) of root collar diameter (RCD) in both *P. edulis* ($r^2 = 0.75$) and *J. osteosperma* ($r^2 = 0.68$). There was no species effect on the relationship between canopy cover and RCD ($P = 0.84$), which allowed us to combine the data and establish a unified RCD–canopy cover allometry ($r^2 = 0.66$; $P < 0.0001$; Fig. 4a). Canopy cover was also a significant predictor of estimated AGB ($P < 0.0001$, log–log relationship) for *P. edulis* ($r^2 = 0.75$), *J. osteosperma* ($r^2 = 0.68$), and combined data ($r^2 = 0.69$; Fig. 4b). The AVIRIS-level AGB spatial patterns could thus be mapped by linking this P–J AGB allometry and the fine-scale remotely sensed PV cover.

Landsat mapping of P–J cover and biomass

A linear regression best described the relationship between PV fractions from AVIRIS and ETM+ ($r^2 = 0.61$; $P < 0.0001$) based upon randomly selected samples ($n = 1500$) from AVIRIS-PV and corresponding ETM-PV pixels (Fig. 5a). Although PV derived from ETM+ was higher than from AVIRIS (slope = 0.66), the relationship lost sensitivity at higher P–J cover. A similar pattern was found between AVIRIS-derived P–

J AGB (Mg/ha) and ETM-PV ($r^2 = 0.52$; $P < 0.0001$; Fig. 5b). The majority of the ETM+ estimates data (60%) were below 10 Mg/ha and most P–J estimates (96%) were below 30 Mg/ha. Based on these regression models, we determined the contemporary P–J cover and AGB for the entire 30 500 km^2 region of P–J woodlands (Fig. 6a, b, respectively).

The regional scale P–J cover map revealed that P–J cover was 27.4% ± 9.9% (mean ± SD), and the P–J AGB was 10.9 ± 4.2 Mg/ha (or 5.2 ± 2.0 Mg C/ha based on the biomass-C conversion coefficient of 0.48; Schlesinger 1997). Based on an estimate of the spatial extent of P–J ecosystems, which is ~27% of the
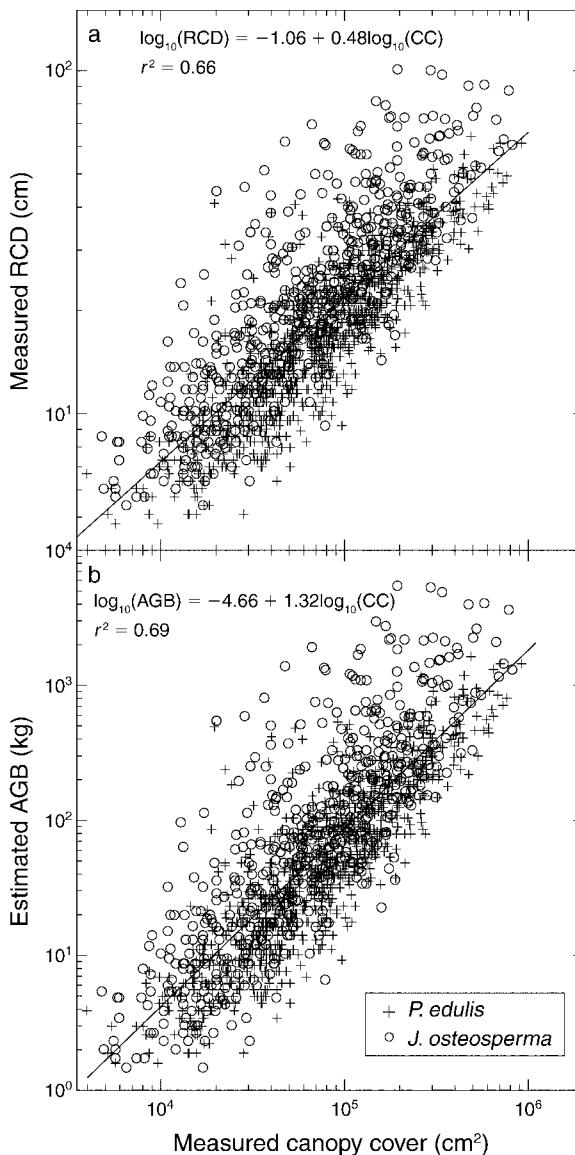
Fig. 4. The unified allometry of (a) measured root collar diameter (RCD), and (b) estimated aboveground biomass (AGB) based on field-measured canopy cover of *Pinus edulis* ($n = 889$) and *Juniperus osteosperma* ($n = 561$).
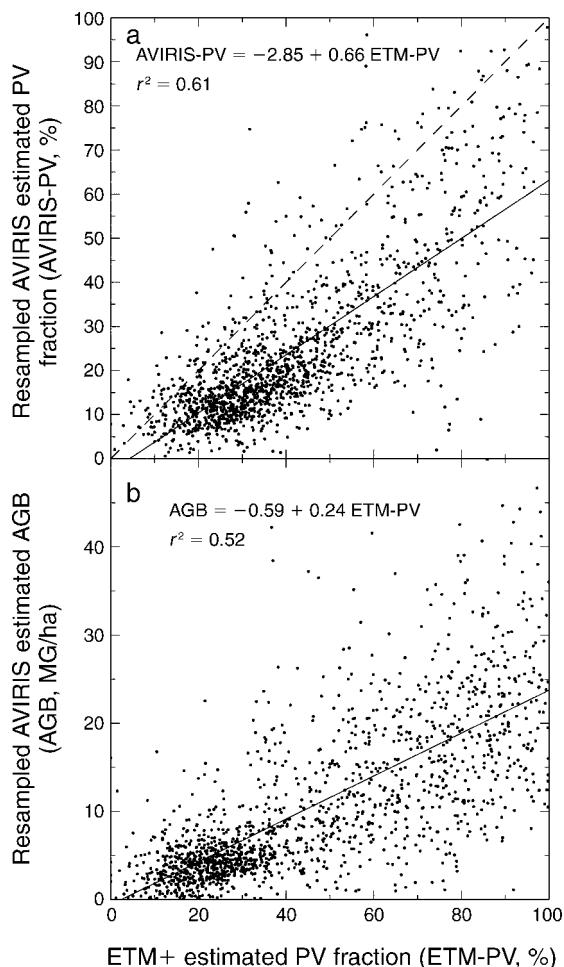
FIG. 5. The relationships between Enhanced Thematic Mapper Plus (ETM+) estimated dry-season photosynthetic vegetation cover fraction (ETM-PV) and averaged, resampled Airborne Visible/Infrared Imaging Spectrometer (AVIRIS) derived (a) PV fraction (AVIRIS-PV) and (b) aboveground biomass (AGB). Approximately 0.5% of pixels ($n = 1500$) were randomly selected for the regression analyses. The dashed line in panel (a) represents a 1:1 relationship.

Colorado Plateau (113 600 km^2; Lowry et al. 2007), we estimate the current-day total P–J woody C stock at 59.0 ± 22.7 Tg C for the entire Colorado Plateau.

Validation of remote-sensing estimates

There was strong agreement ($P < 0.0001$) between our large region P–J cover estimate (Fig. 6a) and both the ReGAP ($r = 0.48$; $n = 428$) and LANDFIRE (uncertainty coefficient = 0.08; $n = 8500$) databases. The mean biases were subtle (ReGAP = −4% and LANDFIRE = −0.7%), and mean absolute errors for ReGAP and LANDFIRE were moderate (9% and 15%, respectively; Table 1). Deviations (underestimates) were amplified in high tree-cover classes (e.g., >60%). A comparison of mean AGB between our remote-sensing estimates and field observations from Grier et al. (1992) showed that

field data were significantly higher than AGB derived from ETM-PV and AVIRIS-PV (ETM-PV = 10.9 Mg/ha; AVIRIS-PV = 17.3 Mg/ha; field observations = 37.9 Mg/ha).

Multiscale comparison of P–J cover and biomass

An example of P–J cover and AGB estimates from AVIRIS is shown in Fig. 7b, c, respectively; this site was located in Grand Staircase-Escalante National Monument (37.33° N, 112.17° W). The spatial pattern of woody vegetation in P–J woodlands and the contrast between highly vegetated P–J patches and litter-bare soil background can be clearly delineated using this high spatial–spectral airborne sensor by referring to a small-scale, very fine spatial resolution (1 m) DOQ acquired in 2006 (Fig. 7a). In contrast, P–J cover and AGB derived from ETM-PV (Fig. 7d, e, respectively) generated "smoothed" vegetation surfaces, which still revealed the general pattern of woody vegetation but lost the heterogeneous spatial arrangement of P–J patches.

Mean P–J cover (25.6%) estimated from AVIRIS-PV for the national parks and the national monument was slightly lower than that from ETM-PV (27.4%) for the entire study site (Fig. 1). However, AGB of AVIRIS (17.3 Mg/ha) estimate was ~37% greater than that derived from ETM-PV (10.9 Mg/ha). In addition, the variation (SD) of AVIRIS estimates (cover = 26.9%; AGB = 11.8 Mg/ha) was significantly higher than ETM+ estimates (cover = 9.9%; AGB = 4.2 Mg/ha).

P–J spatial variation and topography

For the clarity and simplicity of presenting the relationships between P–J spatial abundance and topography, we partitioned the ETM+ scale P–J cover and AGB into equal-interval classes (Fig. 8). The data revealed a tendency of increasing P–J cover and AGB along elevation gradients, but spatial variations among these elevation groups were quite similar. In contrast, the abundance of P–J cover and AGB could not be clearly discerned across slope gradients, but there seemed to be high variations (SD) on steeper slopes. There were no apparent trends of P–J abundance and spatial variation among different aspect classes, although P–J might yield slightly higher mean P–J cover on the north-facing (and perhaps west-facing) slope (Fig. 8f). However, variations among aspect classes were substantial and obscured the differences. Remotely sensed data provide a large number of samples (almost 34×10^6 pixels in our case), and uncertainties become negligible after taking the sample size into account. Therefore, we do not report statistical significance here.

DISCUSSION

Pinyon–juniper cover and biomass on the Colorado Plateau

Spatial patterns of woody cover and biomass are central to understanding ecosystem dynamics and the C cycle. At the regional scale, there were only a limited

a

Projected
cover (%)

100

0

b

AGB
(MG/ha)

49

0
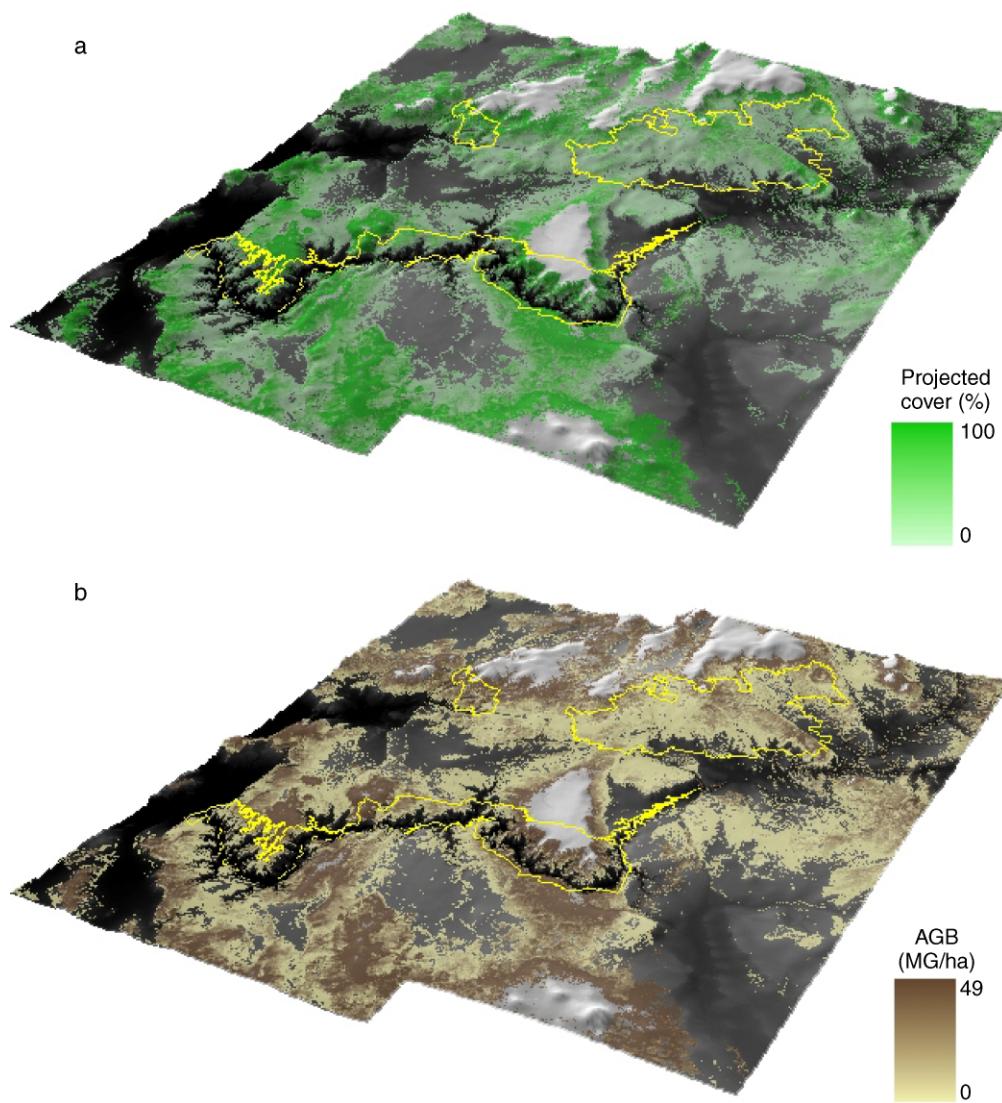
Fig. 6.   Three-dimensional views of regional-scale estimates of pinyon–juniper (P–J) (a) projected cover and (b) aboveground biomass (AGB) in the Colorado Plateau in order to demonstrate the relationships between P–J abundance and topography. Each side of the study region is about 310 km. The background layer is a digital elevation model, and yellow outlines indicate the boundaries of two national parks and one national monument in southern Utah and northern Arizona (see Fig. 1 for the geography of the study region).

amount of cover and aboveground biomass (AGB) data available for P–J woodlands. Our regional P–J cover (Fig. 6a) was comparable to field-based observations from ReGAP and remote estimates from LANDFIRE. Low biases should permit a general prediction of the mean P–J cover over a vast region using the proposed scaling approach. The absolute errors between our estimate and validation data were usually moderate, but they were more pronounced in high tree-cover classes. However, they only occupied a small portion (≤18%) of the sampled areas (Table 1). In addition, the caveats of validation data sets need to be considered. The sampling approach of ReGAP tree cover was solely based on visual estimation (White et al. 2005), and the

outcomes could be biased due to observer errors. Furthermore, systematic errors could be generated since the spatial pattern of sampled plots was not random (mostly along secondary road networks). The LAND-FIRE project focused on areas with substantial amounts of fuels such as coniferous forests but not P–J woodlands. Low tree-cover areas (1–10%), which are frequently found in drylands, were excluded from the analysis. In addition, the data type of LANDFIRE product was ordinal, which would prevent it from a direct comparison to our continuous P–J cover.

Mean field-based AGB estimates were significantly higher than remote-sensing estimates. Low vegetation surface (bare soils and rock outcrops) can be detected

TABLE 1. Quality assessment (mean biases and absolute errors) of the large regional pinyon–juniper projected cover by comparing to tree-cover data from the field-based southwest Regional Gap Analysis Program (ReGAP; $n = 428$) and remote sensing-based LANDFIRE ($n = 8500$) databases.

Tree-cover class (%)	ReGAP (%)			LANDFIRE (%)		
	Proportion	Bias	Absolute error	Proportion	Bias	Absolute error
1–10	6	13	14			
11–20	9	3	7	32	15	15
21–30	43	−3	7	21	9	10
31–40	24	−5	7	14	2	6
41–50	13	−13	14	9	−5	6
51–60	4	−24	24	6	−15	15
>60	1	−37	37	18	−34	34
Overall		−4	9		−0.7	15

Note: For the 1–10% cover class there are no data in the LANDFIRE database. See *Results: Validation of remote-sensing estimates.*

and excluded by the fine resolution field approach, but might not be discernable at coarser resolutions and could be blended into estimates. This may be the cause of negative relationship between AGB estimates and sampling resolutions. However, we draw no conclusion here due to significantly uneven sample areas (ETM+ = 30 500 km^2; AVIRIS = 234 km^2; field observations = 0.015 km^2), and different juniper species (*J. osteosperma* vs. *J. monosperma*), and sampling strategies (only P–J stands ≥90 years were measured in Grier et al. [1992]). AGB reported in this study can be used as a reference for future studies of estimating P–J AGB in the Colorado Plateau or other similar eco-regions using different data and approaches.

Scaling P–J cover and biomass using remote sensing

Scaling is a technique to study the ecological patterns and processes at different organizational levels (Turner et al. 1989, Levin 1992). The low-altitude AVIRIS sensor collected high spatial and spectral resolution images, which made it possible to more fully describe the abundance (field P–J cover; Fig. 3) and surface heterogeneity of P–J woodlands at the crown/patch level (Fig. 7b, c) with high spatial contrasts (SD of cover = 26.9%; SD of AGB = 11.8 Mg/ha). Therefore, AVIRIS-PV derived from automated Monte Carlo unmixing (AutoMCU) can be treated as hundreds of square kilometers of "ground truth," which provides wide range and a sufficient amount of samples for estimating P–J cover and AGB at a large scale by correlating to ETM-PV (Fig. 5).

At the large region scale, ETM-PV represented the average vegetation cover but failed to capture the details (e.g., tree individuals and patches) of P–J systems as indicated by the relatively low spatial variation, and its spatial pattern may not be entirely coherent to AVIRIS (Fig. 7). The relationships between ETM-PV-derived and AVIRIS-derived P–J cover/AGB can be explained by linear regression models (Fig. 5), especially when ETM-PV was low (<40%). However, the trends became less predictable in areas with high P–J vegetation

(>60%). The uncertainty could be explained by the shadow variability contributed from tree canopies, especially in settings with high P–J cover that can substantially influence green vegetation signals (Spanner et al. 1990). The result also showed that ETM-PV was higher than AVIRIS-PV regardless of the abundance of P–J cover (Fig. 5a; comparing to the 1:1 dashed line); Asner and Heidebrecht (2002) had found a similar pattern in the Chihuahuan Desert. Since there was strong agreement between field observations and AVIRIS-PV (Fig. 3), we concluded that ETM-PV was overestimated. This might be due to signal contamination from backgrounds of litter and soils (van Leeuwen and Huete 1996), which were very difficult to unravel with only one shortwave-infrared band available from ETM+. We also found that there were opposite trends of P–J cover and AGB estimates from AVIRIS to ETM+. This could be the result of the nature of nonlinear conversion from cover to AGB (Fig. 4b) and/or scaling discontinuities across sensors. In the future, it would be important to assess the loss of information in dryland vegetation due to pixel size aggregation and spectral convolution across sensors.

Applications for studies of ecological processes

House and Hall (2001) and House et al. (2003) suggested protocols to study ecological processes in arid/semiarid woodlands and grasslands, which require observations across environmental gradients over large spatial extents. This work is not only labor intensive and time consuming, but it is often economically impractical to conduct using conventional field and airborne approaches. Analyzing large-scale spatial patterns of P–J cover and AGB derived from this study with additional information from spatial layers of soils and management practices would provide opportunities to address these issues.

Our results (Fig. 8) suggested that P–J woodlands in the Colorado Plateau yielded higher cover and AGB at higher elevation, which may result from orographic effects of increasing precipitation with elevation (Daly et
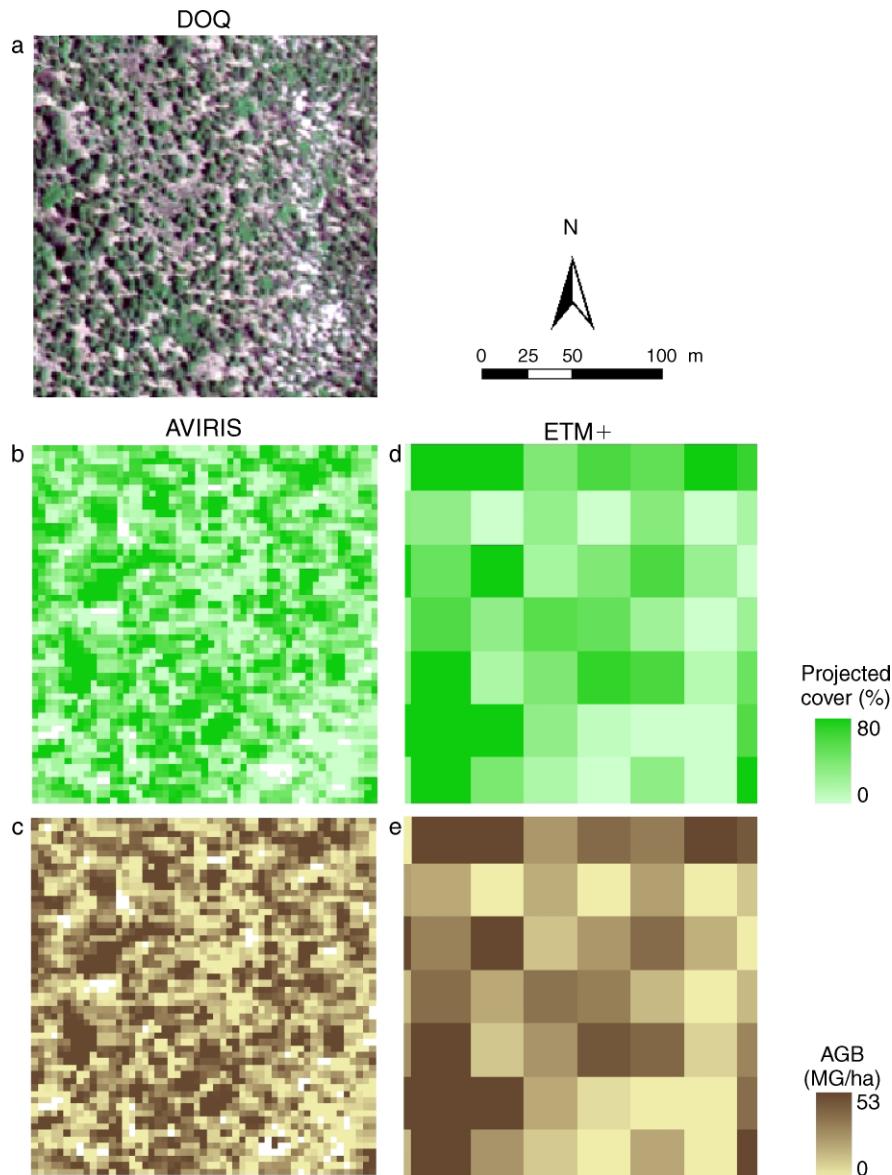
FIG. 7. (a) A close look at pinyon–juniper (P–J) vegetation using a 1-m digital orthophoto quadrangle (DOQ) false-color composite. The green pixels indicate P–J canopy. (b–e) Projected cover (green) and aboveground biomass, AGB, (brown) remote-sensing estimates at resolutions of 3.6 m for AVIRIS (small squares) and 30 m for Enhanced Thematic Mapper Plus (ETM+; large squares).

al. 1994). A similar pattern was also found in previous field studies conducted in similar settings (Padien and Lajtha 1992, Lajtha and Getz 1993). We also found high variations of P–J cover and AGB on steep slopes, which might be the result of several factors such as the higher woody plant mortality on hillslopes with more stressed conditions (e.g., shallow soils, high soil moisture variation, and pronounced soil erosivity; McAuliffe 1994) and/or near-vertical viewing angles of sensors distorting estimates. P–J woodlands produced the highest level of cover on north-facing class, which might be due to the wetter and cooler microclimate in the Northern Hemisphere (Whittaker 1956, 1960). Note that

further statistical adjustments are required for drawing conclusions about topographical effects on P–J wood-lands. For example, random stratified sampling should be applied prior to topographical class comparisons in order to minimize the effects of differing sample sizes and spatial autocorrelation (Aubry and Debouzie 2000). Moreover, other topography-related factors (e.g., water balance parameters such as precipitation, potential evapotranspiration; Kerkhoff et al. 2004), substrate complexity and landforms, anthropogenic/natural per-turbations (e.g., grazing, brush management, tree dieback, prescribed/wild fire), and interactions of these factors should also be taken into account. These
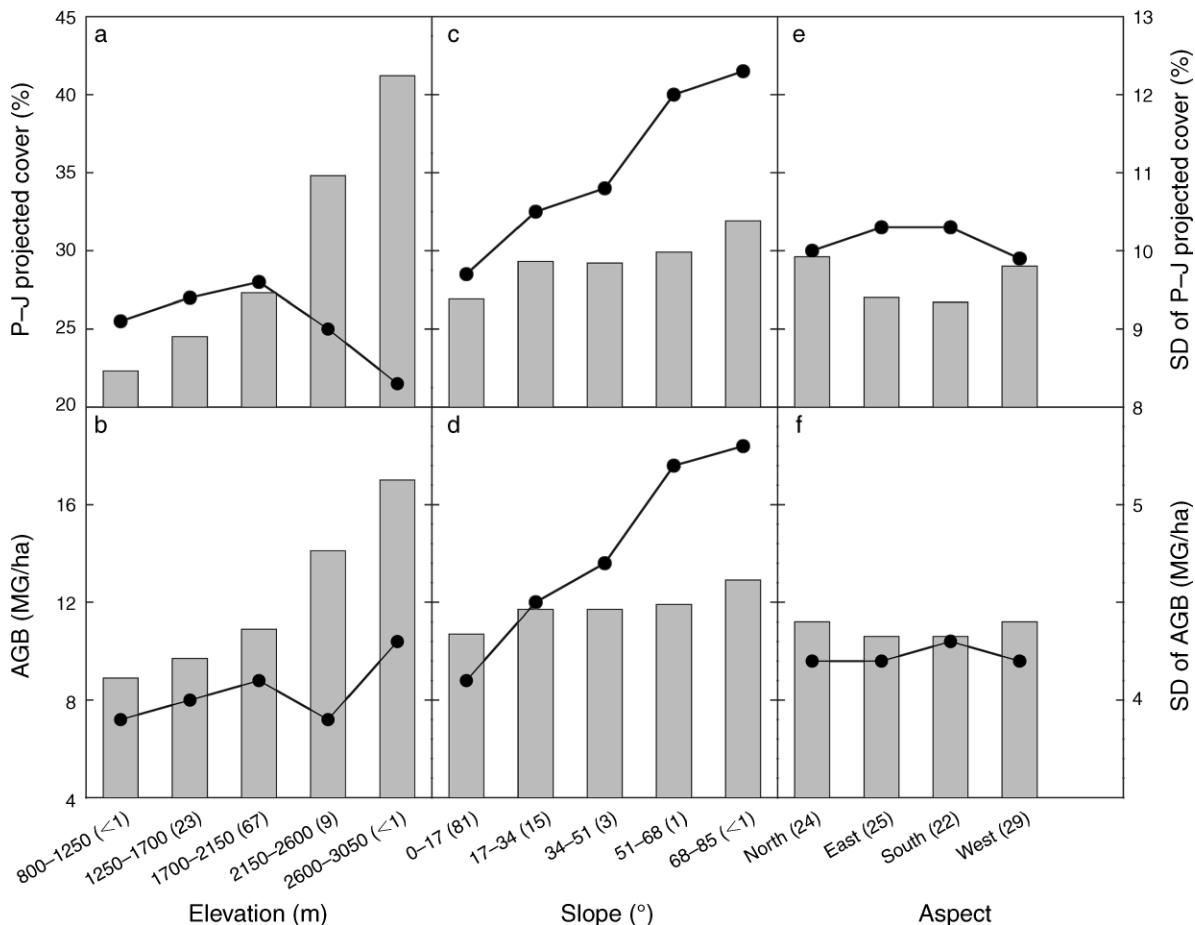
FIG. 8. Mean pinyon and juniper (P–J) projected cover and aboveground biomass (AGB) (shown on the left *y*-axes) partitioned by (a, b) elevation, (c, d) slope, and (e, f) aspect, using equal intervals (*x*-axes; the percentage of each class is given in parentheses). The solid circles are standard deviations (SD, shown on the right *y*-axes) for these cover and AGB groups.

advanced analyses are beyond the scope of this study, but they do represent future research directions.

Limitations and future directions

It is challenging to estimate P–J cover and AGB using a two-dimensional (2-D) imaging approach due to the heterogeneity of woody structural characteristics in dryland ecosystems. We believe that coupling high fidelity, fine spatial/spectral resolution AVIRIS data with a fully automated spectral unmixing algorithm (AutoMCU) may be one of the most robust 2-D approaches to estimate cover and biomass of P–J. Nevertheless, this approach might overestimate AGB at the individual tree scale if two or more small trees were located within one small AVIRIS pixel (13 m^2). This is caused by the nonlinearity (log–log) of the canopy cover–AGB relationship, which is commonly found in P–J and other dryland ecosystems (Fig. 4b; Northup et al. 2005, Huang et al. 2007). In contrast, AGB might be underestimated if the canopy size of an individual tree is greater than the pixel size. However, these uncertain-

ties might not be crucial in the studied region. The distribution of P–J trees was relatively sparse compared to the AVIRIS pixel dimension, even on a high P–J density undisturbed mesa (45.4 ± 9.7 m^2 [mean ± SD] per individual; see examples in Fig. 7a and in Harris et al. [2003]). Therefore, the case of overestimation may only rarely occur. In addition, our extensive field observations (*n* = 1450) show that the majority (73%) of *P. edulis* and *J. osteosperma* canopies are encompassed by the AVIRIS pixel size used in this study. Hence, the effects of underestimation should be moderate. In the future, these aforementioned uncertainties could be minimized by integrating high spatial–spectral resolution AVIRIS with airborne lidar (light detecting and ranging; Asner et al. 2007). This latest technique can provide a unique 3-D perspective (cover + height) of dryland vegetation, which would be correlated with AGB.

POTENTIAL OF RESEARCH AND MANAGEMENT IMPLICATIONS

This study demonstrated the feasibility of scaling up P–J cover and AGB to the large, regional level by

correlating field measurements, allometric equations, and airborne imaging spectroscopy and multispectral ETM+ observations. An even larger regional mapping of P–J cover and AGB in North America could potentially be produced by integrating the allometric models of dominant tree species in other P–J systems (e.g., the Great Basin and Mogollon Rim; West 1999), including *P. monophylla* and *J. monosperma* (Miller et al. 1981, Grier et al. 1992, Jenkins et al. 2003), using the demonstrated approach. By referring to ReGAP (Lowry et al. 2007), the tree cover and AGB in 200 000 km^2 P–J systems in five states (AZ, CO, NM, NV, UT) of the southwest United States could also be generated. Systematic mapping of P–J woodlands using satellite images would facilitate the monitoring of vegetation dynamics (e.g., P–J die-off due to drought and beetle infestation; Breshears et al. 2005, Shaw et al. 2005) over this broad region. More generally, the study is of interest because the proposed synoptic sensing approaches could be adapted to other dryland ecosystems of similar vegetation structures such as mesquite and oak woodlands.

From a management perspective, large-scale mapping of P–J cover and biomass would facilitate decision making for continental-scale and global-scale C management programs such as the North American Carbon Program (information *available online*).[11] The primary aim of the program is to investigate the storage and fluxes of C pools through time in North America and in adjacent ocean regions. This study provides information to the program in the following areas:

1) Large-scale contemporary time-series P–J abundance estimates derived from remotely sensed data can help determine the emissions and uptake of greenhouse gases (e.g., CO_2, CH_4, CO) in the P–J ecosystems of North America, with further aids from field observations, experiments, and ecosystem modeling techniques (Field et al. 1995, Asner et al. 2005b, Huang et al. 2008).

2) Dryland ecosystem processes are complex, and the abundance of woody C can be influenced by many factors such as climate, disturbance regimes, and management (Burgess 1995, Scholes and Archer 1997, Klausmeier 1999, Sankaran et al. 2004, 2005). Coupling the large-scale P–J cover and AGB maps with other spatial layers such as topography (demonstrated in this paper, Fig. 8), edaphic complexity (soils and landforms), and land tenures (private ranch vs. federal protected parks and monuments) would facilitate understanding of drivers that regulate the P–J ecosystem processes for North America.

3) Accurately estimated P–J cover and AGB are essential for constraining ecosystem models to actual conditions to provide quantitative simulations of C fluxes and forecast scenarios of P–J ecosystem dynamics in these extensive dryland ecosystems.

[11] ⟨http://www.nacarbon.org/nacp/⟩

LITERATURE CITED

Adams, J. B., M. O. Smith, and A. R. Gillespie. 1993. Imaging spectroscopy: interpretation based on spectral mixture analysis. Pages 145–166 *in* C. M. Pieters and P. A. Englert, editors. Remote geochemical analysis: elemental and mineralogical composition. Cambridge University Press, New York, New York, USA.

Archer, S. 1993. Vegetation dynamics in changing environments. Rangelands Journal 15:104–116.

Archer, S., D. S. Schimel, and E. A. Holland. 1995. Mechanisms of shrubland expansion: land use, climate or CO_2? Climatic Change 29:91–99.

Asner, G. P. 1998. Biophysical and biochemical sources of variability in canopy reflectance. Remote Sensing of Environment 64:234–253.

Asner, G. P., S. Archer, F. R. Hughes, J. R. Ansley, and C. A. Wessman. 2003a. Net changes in regional woody vegetation cover and carbon storage in Texas drylands, 1937–1999. Global Change Biology 9:316–335.

Asner, G. P., M. M. C. Bustamante, and A. R. Townsend. 2003b. Scale dependence of biophysical structure in deforested lands bordering the Tapajós National Forest, Central Amazon. Remote Sensing of Environment 87:507–520.

Asner, G. P., A. J. Elmore, L. P. Olander, R. E. Martin, and A. T. Harris. 2004. Grazing systems, ecosystem responses, and global change. Annual Review of Environment and Resources 29:261–299.

Asner, G. P., and K. B. Heidebrecht. 2002. Spectral unmixing of vegetation, soil and dry carbon cover in arid regions: comparing multispectral and hyperspectral observations. International Journal of Remote Sensing 23:3939–3958.

Asner, G. P., and K. B. Heidebrecht. 2005. Desertification alters regional ecosystem–climate interactions. Global Change Biology 11:182–194.

Asner, G. P., M. Keller, J. N. Silva, D. E. Knapp, E. N. Broadbent, and P. J. C. Oliveira. 2005a. Selective logging in the Brazilian Amazon. Science 310:480–482.

Asner, G. P., D. E. Knapp, A. N. Cooper, M. C. C. Bustamante, and L. O. Olander. 2005b. Ecosystem structure throughout the Brazilian Amazon from Landsat data and spectral unmixing. Earth Interactions 9:1–31.

Asner, G. P., D. E. Knapp, T. Kennedy-Bowdoin, M. O. Jones, R. E. Martin, J. Boardman, and C. B. Field. 2007. Carnegie Airborne Observatory: in-flight fusion of hyperspectral imaging and waveform light detection and ranging (wLiDAR) for three-dimensional studies of ecosystems. Journal of Applied Remote Sensing 1:013537.

Asner, G. P., and D. B. Lobell. 2000. A biogeophysical approach for automated SWIR unmixing of soils and vegetation. Remote Sensing of Environment 74:99–112.

Asner, G. P., J. L. Privette, C. A. Wessman, and A. C. Bateson. 2000. Impact of tissue, canopy, and landscape factors on the hyperspectral reflectance variability of arid ecosystems. Remote Sensing of Environment 74:69–84.

Aubry, P., and D. Debouzie. 2000. Geostatistical estimation variance for the spatial mean in two-dimensional systematic sampling. Ecology 81:543–553.

Augustine, D. J., and S. J. McNaughton. 2004. Regulation of shrub dynamics by native browsing ungulates on East African rangeland. Journal of Applied Ecology 41:45–58.

Barbosa, R. I., and P. M. Fearnside. 2005. Above-ground biomass and the fate of carbon after burning in the savannas of Roraima, Brazilian Amazonia. Forest Ecology and Management 216:295–316.

Barney, M. A., and N. C. Frischknecht. 1974. Vegetation changes following fire in the pinyon–juniper type of west-central Utah. Journal of Range Management 27:91–96.

Bateson, A. C., G. P. Asner, and C. A. Wessman. 2000. Endmember bundles: a new approach to incorporating endmember variability into spectral mixture analysis. IEEE Transactions on Geoscience and Remote Sensing 38:1083–1094.

Ben-Shahar, R. 1998. Changes in structure of savanna woodlands in northern Botswana following the impacts of elephants and fire. Plant Ecology 136:189–194.

Bond, W. J., and J. J. Midgley. 2001. Ecology of sprouting in woody plants: the persistence niche. Trends in Ecology and Evolution 16:45–51.

Bradley, B. A., R. A. Houghton, J. F. Mustard, and S. P. Hamburg. 2006. Invasive grass reduces aboveground carbon stocks in shrublands of the Western U.S. Global Change Biology 12:1815–1822.

Branson, A. 1985. Vegetation changes on western rangelands. Range Monograph 2:1–75.

Breshears, D. D., et al. 2005. Regional vegetation die-off in response to global-change-type drought. Proceedings of the National Academy of Sciences (USA) 102:15144–15148.

Brus, D. J., and J. J. DeGruijter. 1993. Design-based versus model-based estimates of spatial means: theory and application in environmental soil science. Environmetrics 4:123–152.

Buffington, L. C., and C. H. Herbel. 1965. Vegetational changes on semidesert grassland range from 1858 to 1963. Ecological Monographs 35:139–164.

Burgess, T. L. 1995. Desert grassland, mixed shrub savanna, shrub steppe, or semidesert scrub: The dilemma of coexisting growth forms. Pages 31–67 in M. McClaran and T. R. Van Devender, editors. The desert grassland. University of Arizona Press, Tucson, Arizona, USA.

Canfield, R. H. 1941. Application of the line intercept method of sampling range vegetation. Journal of Forestry 39:388–394.

Chojnacky, D. C. 1991. Growth prediction for Arizona's mesquite (Prosopis velutina) woodlands. Forest Ecology and Management 42:293–310.

Daly, C., R. P. Neilson, and D. L. Phillips. 1994. A statistical–topographic model for mapping climatological precipitation over mountainous terrain. Journal of Applied Meteorology 33:140–158.

Darling, M. L. S. 1967. Structure and productivity of a pinyon–juniper woodland in northern Arizona. Dissertation. Duke University, Durham, North Carolina, USA.

Field, C. B., J. T. Randerson, and C. M. Malmström. 1995. Global net primary production: combining ecology and remote sensing. Remote Sensing of Environment 51:74–88.

Gholz, H. L. 1982. Environmental limits on aboveground net primary production, leaf area, and biomass in vegetation zones of the Pacific Northwest. Ecology 63:469–481.

Glendening, G. E. 1952. Some quantitative data on the increase of mesquite and cactus on a desert grassland range in Southern Arizona. Ecology 33:319–328.

Goslee, S. C., K. M. Havstad, D. P. C. Peters, A. Rango, and W. H. Schlesinger. 2003. High-resolution images reveal rate and pattern of shrub encroachment over six decades in New Mexico, U.S.A. Journal of Arid Environments 54:755–767.

Gray, S. T., J. L. Betancourt, S. T. Jackson, and R. G. Eddy. 2006. Role of multidecadal climate variability in a range extension of pinyon pine. Ecology 87:1124–1130.

Green, R. O., M. L. Eastwood, C. M. Sarture, T. G. Chrien, M. Aronsson, B. J. Chippendale, J. A. Faust, B. E. Pavri, C. J. Chovit, and M. Solis. 1998. Imaging spectroscopy and the airborne visible/infrared imaging spectrometer (AVIRIS). Remote Sensing of Environment 65:227–248.

Grier, C. C., K. J. Elliott, and D. G. McCullough. 1992. Biomass distribution and productivity of Pinus edulis–

Juniperus monosperma woodlands of north-central Arizona. Forest Ecology and Management 50:331–350.

Gruijter, J. J., and C. J. F. Braak. 1990. Model-free estimation from spatial samples: a reappraisal of classical sampling theory. Mathematical Geology 22:407–415.

Harris, A. T., G. P. Asner, and M. E. Miller. 2003. Changes in vegetation structure after long-term grazing in pinyon–juniper ecosystems: integrating imaging spectroscopy and field studies. Ecosystems 6:368–383.

Hibbard, K. A., S. Archer, D. S. Schimel, and D. W. Valentine. 2001. Biogeochemical changes accompanying woody plant encroachment in a subtropical savanna. Ecology 82:1999–2011.

Houghton, R. A., J. L. Hackler, and K. T. Lawrence. 1999. The U.S. carbon budget: contributions from land-use change. Science 285:574–578.

House, J. I., S. Archer, D. D. Breshears, and R. J. Scholes. 2003. Conundrums in mixed woody–herbaceous plant systems. Journal of Biogeography 30:1763–1777.

House, J. I., and D. O. Hall. 2001. Productivity of tropical savannas and grasslands. Pages 363–400 in J. Roy, B. Saugier, and H. A. Mooney, editors. Terrestrial global productivity. Academic Press, San Diego, California, USA.

Huang, C., S. E. Marsh, M. McClaran, and S. Archer. 2007. Postfire stand structure in a semiarid savanna: cross-scale challenges estimating biomass. Ecological Applications 17:1899–1910.

Huang, M., G. P. Asner, M. Keller, and J. A. Berry. 2008. An ecosystem model for tropical forest disturbance and selective logging. Journal of Geophysical Research 113:G01002.

Huenneke, L. F., J. P. Anderson, M. Remmenga, and W. H. Schlesinger. 2002. Desertification alters patterns of aboveground net primary production in Chihuahuan ecosystems. Global Change Biology 8:247–264.

Hughes, R. F., S. R. Archer, G. P. Asner, C. A. Wessman, C. McMurtry, J. Nelson, and R. J. Ansley. 2006. Changes in aboveground primary production and carbon and nitrogen pools accompanying woody plant encroachment in a temperate savanna. Global Change Biology 12:1733–1747.

Jackson, R. B., J. L. Banner, E. G. Jobbágy, W. T. Pockman, and D. H. Wall. 2002. Ecosystem carbon loss with woody plant invasion of grasslands. Nature 418:623–626.

Jenkins, J. C., D. C. Chojnacky, L. S. Heath, and R. A. Birdsey. 2003. National-scale biomass estimators for United States tree species. Forest Science 49:12–35.

Kerkhoff, A. J., S. N. Martens, G. A. Shore, and B. T. Milne. 2004. Contingent effects of water balance variation on tree cover density in semiarid woodlands. Global Ecology and Biogeography 13:237–246.

Klausmeier, C. A. 1999. Regular and irregular patterns in semiarid vegetation. Science 284:1826–1828.

Lajtha, K., and J. Getz. 1993. Photosynthesis and water-use efficiency in pinyon–juniper communities along an elevation gradient in northern New Mexico. Oecologia 94:95–101.

Levin, S. A. 1992. The problem of pattern and scale in ecology: the Robert H. MacArthur award lecture. Ecology 73:1943–1967.

Lowry, J., et al. 2007. Mapping moderate-scale land-cover over very large geographic areas within a collaborative framework: a case study of the Southwest Regional Gap Analysis Project (SWReGAP). Remote Sensing of Environment 108:59–73.

Ludwig, J. A., J. F. Reynolds, and P. D. Whitson. 1975. Size–biomass relationships of several Chihuahuan Desert shrubs. American Midland Naturalist 94:451–461.

McAuliffe, J. R. 1994. Landscape evolution, soil formation, and ecological patterns and processes in Sonoran Desert bajadas. Ecological Monographs 64:111–148.

McClaran, M. P., and G. R. McPherson. 1999. Oak savanna of the American Southwest. Pages 275–287 in R. C. Anderson, J. S. Fralish, and J. M. Baskin, editors. Savanna, barrens,

and rock outcrop plant communities of North America. Cambridge University Press, Cambridge, UK.

McPherson, G. R. 1997. Ecology and management of North American savannas. University of Arizona Press, Tucson, Arizona, USA

Miller, E. L., R. O. Meeuwig, and J. D. Budy. 1981. Biomass of singleleaf pinyon and Utah juniper. Intermountain Forest and Range Experimental Station, U.S. Department of Agriculture, Ogden, Utah, USA.

Miller, J. D., S. R. Yool, S. R. Danzer, J. M. Watts, and S. Stone. 2003. Cluster analysis of structural stage classes to map wildland fuels in a Madrean ecosystem. Journal of Environmental Management 68:239–252.

Miller, R. F., and J. A. Rose. 1999. Fire history and western juniper encroachment in sagebrush steppe. Journal of Range Management 52:550–559.

Miller, R. F., and P. E. Wigand. 1994. Holocene changes in semiarid pinyon–juniper woodlands: Response to climate, fire, and human activities in the U.S. Great Basin. BioScience 44:465–474.

Northup, B. K., S. F. Zitzer, S. Archer, C. R. McMurtry, and T. W. Boutton. 2005. Above-ground biomass and carbon and nitrogen content of woody species in a subtropical thorn-scrub parkland. Journal of Arid Environments 62:23–43.

O'Brien, R. A., and S. W. Woudenberg. 1999. Description of pinyon–juniper and juniper woodlands in Utah and Nevada from an inventory perspective. Pages 55–59 in S. B. Monsen and R. Stevens, editors. Proceedings: ecology and management of pinyon–juniper communities within the Interior West. Rocky Mountain Research Station, U.S. Department of Agriculture, Ogden, Utah, USA.

Pacala, S. W., et al. 2001. Consistent land- and atmosphere-based U.S. carbon sink estimates. Science 292:2316–2320.

Padien, D. J., and K. Lajtha. 1992. Plant spatial pattern and nutrient distribution in pinyon–juniper woodlands along an elevational gradient in northern New Mexico. International Journal of Plant Sciences 153:425–433.

Rich, P. M., D. D. Breshears, and A. B. White. 2008. Phenology of mixed woody–herbaceous ecosystems following extreme events: net and differential responses. Ecology 89: 342–352.

Sankaran, M., et al. 2005. Determinants of woody cover in African savannas. Nature 438:846–849.

Sankaran, M., J. Ratnam, and N. P. Hanan. 2004. Tree–grass coexistence in savannas revisited: insights from an examination of assumptions and mechanisms invoked in existing models. Ecology Letters 7:480–490.

Scanlon, T. M., J. D. Albertson, K. K. Caylor, and C. A. Williams. 2002. Determine land surface fractional cover from NDVI and rainfall time series for a savanna ecosystem. Remote Sensing of Environment 82:376–388.

Schimel, D., et al. 2000. Contribution of increasing CO_2 and climate to carbon storage by ecosystems in the United States. Science 287:2004–2006.

Schlesinger, W. H. 1997. Biogeochemistry: an analysis of global change. Second edition. Academic Press, San Diego, California, USA.

Scholes, R. J., and S. R. Archer. 1997. Tree–grass interactions in savannas. Annual Review of Ecology and Systematics 28: 517–544.

Shaw, J. D., B. E. Steed, and L. T. DeBlander. 2005. Forest inventory and analysis (FIA) annual inventory answers the question: What is happening to pinyon–juniper woodlands? Journal of Forestry 103:280–285.

Spanner, M. A., L. L. Pierce, D. L. Peterson, and S. W. Running. 1990. Remote sensing of temperate coniferous forest leaf area index. The influence of canopy closure, understory vegetation and background reflectance. International Journal of Remote Sensing 11:95–111.

Stimson, H. C., D. D. Breshears, S. L. Ustin, and S. C. Kefauver. 2005. Spectral sensing of foliar water conditions in two co-occurring conifer species: *Pinus edulis* and *Juniperus monosperma*. Remote Sensing of Environment 96:108–118.

Tausch, R. J., and R. S. Nowak. 1999. Fifty years of ecotone change between shrub and tree dominance in the Jack Springs pinyon research natural area. Pages 71–77 in E. D. McArthur, W. K. Ostler, and C. L. Wamboldt, editors. Proceedings: shrubland ecotones. Rocky Mountain Research Station, U.S. Department of Agriculture, Ephraim, Utah, USA.

Tucker, C. J., and P. J. Sellers. 1986. Satellite remote sensing for primary production. International Journal of Remote Sensing 7:1395–1416.

Turner, M. G., V. H. Dale, and R. H. Gardner. 1989. Predicting across scales: theory development and testing. Landscape Ecology 3:245–252.

van Leeuwen, W. J. D., and A. R. Huete. 1996. Effects of standing litter on the biophysical interpretation of plant canopies with spectral indices. Remote Sensing of Environment 55:123–138.

Vermote, E. F., D. Tanré, J. L. Deuzé, M. Herman, and J. J. Morcrette. 1997. Second simulation of the satellite signal in the solar spectrum: an overview. IEEE Transactions on Geoscience and Remote Sensing 35:3675–3686.

Weisberg, P. J., E. Lingua, and R. B. Pillai. 2007. Spatial patterns of pinyon–juniper woodland expansion in Central Nevada. Rangeland Ecology and Management 60:115–124.

West, N. E. 1999. Juniper–piñon savannas and woodlands of western North America. Pages 288–308 in R. C. Anderson, J. S. Fralish, and J. M. Baskin, editors. Savanna, barrens, and rock outcrop plant communities of North America. Cambridge University Press, Cambridge, UK.

White, M. A., J. D. Shaw, and R. D. Ramsey. 2005. Accuracy assessment of the vegetation continuous field tree cover product using 3954 ground plots in the south-western USA. International Journal of Remote Sensing 26:2699–2704.

Whittaker, R. H. 1956. Vegetation of the Great Smoky Mountains. Ecological Monographs 26:1–80.

Whittaker, R. H. 1960. Vegetation of the Siskiyou Mountains, Oregon and California. Ecological Monographs 30:279–338.

Whittaker, R. H., and W. A. Niering. 1975. Vegetation of the Santa Catalina Mountains, Arizona. V. Biomass, production, and diversity along the elevation gradient. Ecology 56:771–790.